

# Improved Supersonic Performance for the F-16 Inlet Modified for the J79 Engine

Louis G. Hunter\* and J.A. Cawthon  
*General Dynamics Corporation, Fort Worth, Texas*

The F-16 inlet modified for the J79-GE-119 engine, the integration of a new inlet incorporated into the F-16A/B airframe, a new inlet bleed system, the design philosophy, development tests, and performance of the inlet throughout the flight and maneuver envelope are reviewed. Model data are included which show the performance of the inlet in terms of pressure recovery, distortion, and turbulence. An engine bypass system was developed for providing cooling air for the hot engine case and exhaust nozzle, to provide good ejector exhaust nozzle performance, and to maintain stable inlet operation at high Mach numbers. The F-16/79 inlet retains the same location, capture area, cross-sectional shape, and duct length. The additions are a longer compression ramp composed of a fixed and curved ramp surface for improved high Mach number performance and a throat slot boundary-layer control for reduced shock interaction. These improvements provide a 20% increase in pressure recovery and 60% decrease in spill drag at Mach 2.0.

## Introduction

THE F-16/79 aircraft is a tailored version of the operational F-16A/B. The F-16/79 demonstrator recently completed a rigorous flight development certification program with USAF surveillance and participation. This development program integrated an improved version of the proven GE J79 engine into the F-16 aircraft, which required a new inlet to be incorporated into the basic F-16 structure and systems.

The F-16/79 is a single-engine tactical fighter with air-to-air combat capabilities. The aircraft is powered by a 17,820 lb thrust J79-GE-119 turbojet engine. An airframe-mounted accessory drive gearbox powers aircraft accessories, and a jet-fuel starter provides self-starting of the engine. Recently, in a quick-reaction simulated intercept mission, the F-16/79 demonstrated its scramble capability by going from a cold start, with no ground power, to 40,000 ft and twice the speed of sound in 6 min, 11 s. A major design milestone in the inlet/engine integration of this airplane modification was to develop a new multiple ramp inlet with a sophisticated bleed system which would enable this airplane to operate and easily accelerate to  $M=2.0+$ . The purpose of this paper is to describe the design, validation, and performance process through three wind tunnel tests and a flight test.

## Overview of the Inlet Design

A cross section of the F-16/79 inlet and duct as installed in the development aircraft is shown and compared with the F-16 inlet and duct in Fig. 1. The new inlet design utilizes the present F-16A/B inlet cowl and subsonic duct so that external nacelle lines are not changed aft of fuselage station (F.S.) 160 in. (F.S. 160 is the inlet cowl location) and internal lines are not changed aft of F.S. 188. The inlet capture area also remains unchanged at 826.7 in.<sup>2</sup> Supersonic performance is considerably enhanced by the incorporation of a fixed-geometry double compression ramp. The ramp is composed

of a 6 deg initial wedge, followed by an isentropic surface that turns the local flow through an additional 6.67 deg forward of the cowl lip, for a total turn of 12.67 deg. The new double ramp design reduces the throat area approximately 21% compared with the F-16A/B. This approach accomplishes both design and performance goals. First, it provides an efficient means for matching the inlet throat size to the lower airflow requirement of the 119 engine. Second, it turns and compresses the flow in supersonic flight to result in a 20% increase in total-pressure recovery and a 68% decrease in spillage drag at Mach 2.0, compared with the basic F-16 inlet design (see Fig. 2).

Supersonic inlet performance is further enhanced by the use of boundary-layer control (BLC) provided by a transverse boundary-layer-bleed slot located on the ramp near the inlet throat (Fig. 3). Low-energy boundary-layer air is removed through this slot and discharged through flush, aft-facing louvers located on the nacelle shoulders. This BLC system minimizes the degrading effect of shock/boundary-layer interaction, increases subsonic diffuser efficiency, and expands the stable operating range of the inlet at supersonic Mach numbers. The bleed slot design also incorporates a differential-pressure-actuated door that closes the slot and prevents reverse flow during ground and low speed flight operations (Fig. 4).

The inserted compression ramp is terminated at F.S. 188, and from this point back to F.S. 335, F-16 internal duct lines are maintained. Between F.S. 335 and the engine inlet at F.S. 361.5 a reducing transition section is inserted to match the smaller inlet diameter of the -119 engine. Figure 5 shows a comparison of flow area between the F-16 and the F-16/79 ducts. Also shown are enlarged views of the transition duct secondary-flow-system bypass valve mechanism as well as a cross-section of the bypass valve. The duct flow area decrease imposed by the transition section increases local flow velocity forward of the engine, and, along with the low-energy air removal through the bypass valve, results in a decrease in pressure distortion and turbulence at the engine inlet, thus improving installed engine performance.

The bypass valve is the main secondary flow control device. The valve can be positioned either fully open or fully closed or at any intermediate position in response to control signals. When the valve is open, a portion of the primary inlet airflow is bypassed through the exposed annular slot into the nacelle. This bypass air is drawn through the nacelle by the pumping action of the ejector nozzle. This secondary airflow provides

Presented as Paper 84-1272 at the AIAA/SAE/ASME 20th Joint Propulsion Conference, Cincinnati, Ohio, June 11-13, 1984; received Aug. 6, 1984; revision received Oct. 11, 1984. Copyright © 1984 by General Dynamics Corporation. Published by the American Institute of Aeronautics and Astronautics with permission.

\*Engineering Specialist, Member AIAA.

†Engineering Specialist, Senior.

engine cooling air as well as enhanced gross thrust as the cool air mixes with the primary jet. At higher flight speeds (above Mach 0.7 the valve pressure differential is sufficiently high to schedule the bypass valve in the open position, which provides additional airflow at the high Mach numbers and additional stability margin.

### Preliminary Inlet Design Considerations

Since the maximum inlet airflow (engine plus bypass) was approximately 83% of the F-100 engine airflow, a corresponding inlet throat reduction from 713 in.<sup>2</sup> (which is the F-16A/B inlet throat area) to 594 in.<sup>2</sup> was chosen as one of the primary test configurations. This configuration was designed with a 6-deg fixed first ramp and fixed second ramp with a curved isentropic surface which turns the flow through an additional 5 deg (see Fig. 6). Along with this configuration are shown two additional designs, each with a Mach 2.0 shock system superimposed.

Configuration 1 was designed for operation at Mach 1.8 with minimum overspeed capability. Configurations 1 and 24 were designed for operation at Mach 2 with some overspeed capability. Thus, at Mach 2.0, the shock system on configuration 1 focuses inside the cowl lip, while the other two longer ramp configurations focus the shock system outside the cowl lip. All configurations provided stable operation at Mach 2, but configurations 12 and 24 resulted in an increase in stability margin. Table 1 shows these three basic inlet configurations to be tested, along with other features such as variations in the BLC system, throat size, duct smoothing, vortex generators, and sideplate variations. This test matrix was tested in the NASA Ames 6 × 6 ft wind tunnel.

At the conclusion of this first wind tunnel test, it was determined that configuration 12 was the most promising design. Vortex generators, sideplate cutback, and aft-ramp fill (smoothing the F.S. 188 inlet discontinuity) did not make a significant difference in inlet performance and distortion, and were discarded.

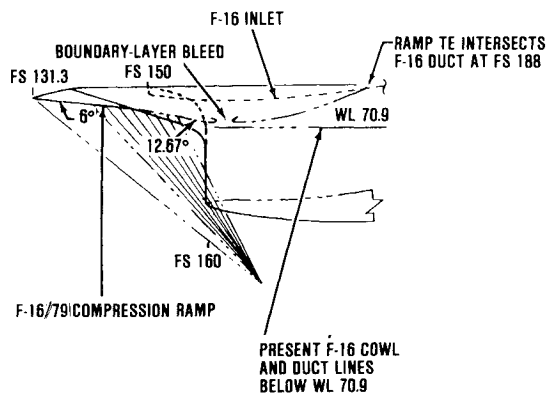
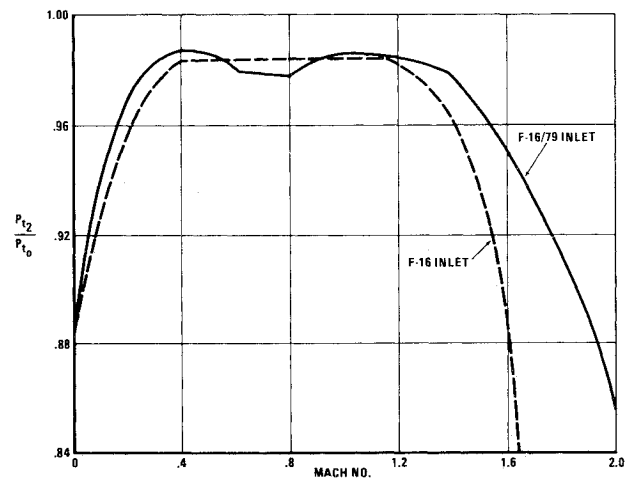
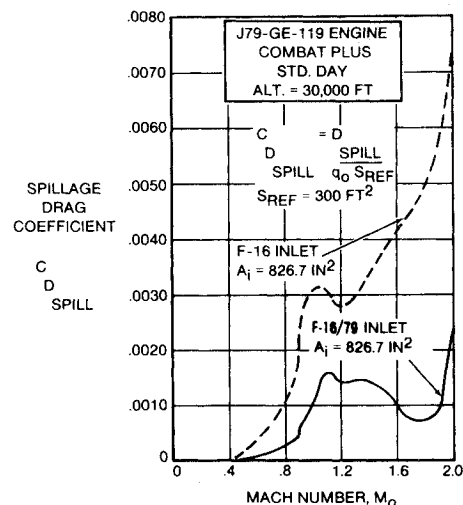


Fig. 1 F-16/79 compression ramps.

During the NASA Ames test it was discovered that the bleed system was marginal at high Mach numbers and at the low Mach numbers a reverse flow was coming back through the bleed system, causing flow separation in the throat slot region. Therefore, a second test was set up at the General Dynamics Engineering Test Laboratory (GD/ETL) to improve the bleed flow system and develop a set of bleed characteristic curves for the bleed louvers. In addition to the above requirements, this test also served to determine the static performance of the inlet. This test was designated the static model test. It was during this test that the pressure



a) Inlet pressure recovery comparison.



b) Inlet spillage drag comparison.

Fig. 2 F-16 and F-16/79 performance comparisons.

Table 1 F-16/79 inlet design characteristics

Configuration No.	Ramp leading-edge fuselage station, in.	Throat size, in. <sup>2</sup>	Type BLC	Sideplate Configuration	$\theta_R$ , deg	Subsonic ramp	VG's
1	134.3	594	Throat slot	Solid	6-11	Basic	None
2	134.3	594	Throat slot	Slotted	6-11	Basic	None
14	134.3	594	Throat slot and porous plate	Solid	6-11	Basic	None
12	131.3	562.4	Throat slot	Solid	6-12.67	Basic	None
15	131.3	562.4	Throat slot	Solid	6-12.67	Basic	Yes
21	131.3	562.4	Throat slot	Solid	6-12.67	Filled	None
22	131.3	562.4	Throat slot	Solid	6-12.67	Filled	Yes
23	131.3	562.4	None-taped slot	Solid	6-12.67	Filled	Yes
24	130	563	Throat slot	Solid	6-12.67	Basic	None

differential throat slot door (Fig. 4) was developed to prevent the reverse flow in the throat slot.

From the results of the NASA Ames and GD/ETL tests, a final wind tunnel test was formulated to test configuration 12 with a more elaborate bleed system including a louver exhaust system (Fig. 7). This configuration has five bleed cavities on the ramp which are bled outwardly through the louvers and centrally through the diverter chamber to the three rear chambers. This final configuration was tested at the Rockwell 7 × 7 ft Trisonic Facility. After a comparison of results, which

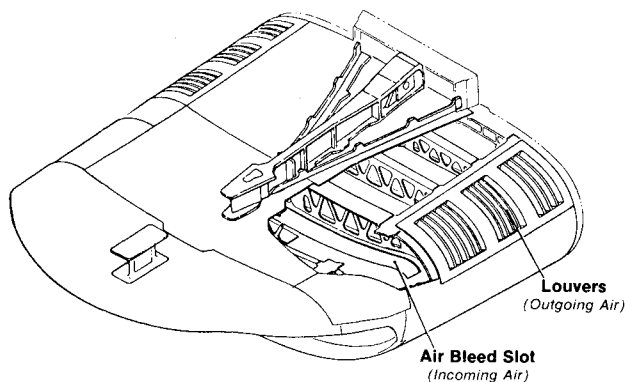


Fig. 3 Internal view of the model F-16/79 inlet.

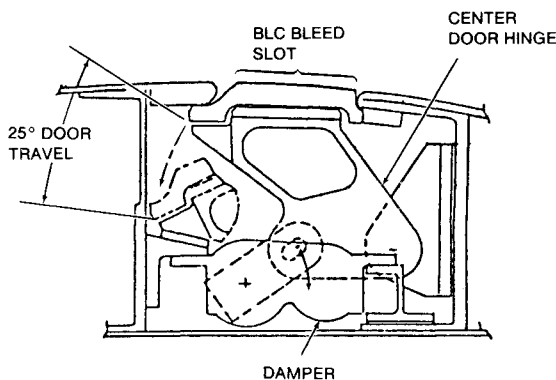


Fig. 4 Inlet/slot boundary-layer bleed closure door/damper.

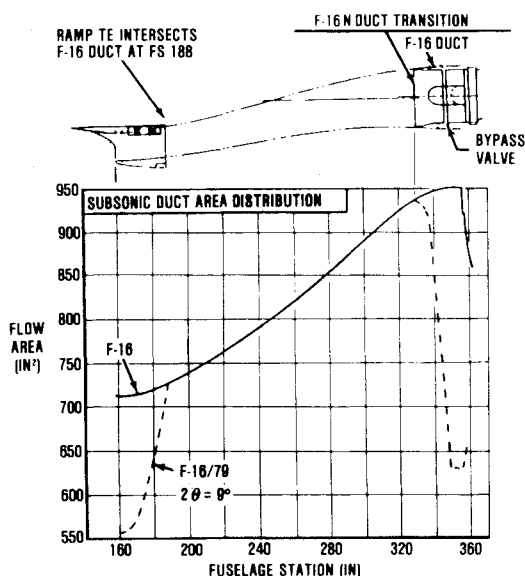


Fig. 5 F-16/79 inlet duct area distribution and transition duct and bypass valve arrangement.

will be discussed in detail in the section of Wind Tunnel Results, it was determined that a single throat slot bleed (chamber 5) flowing outward through the louvers and centrally through the diverter through chambers 6 and 7 would be adequate for the Mach 2.0 requirement. This was confirmed by the flight test series, which verified that this final configuration was more than adequate to provide the necessary operating flow margins for Mach 2.0 flight.

### Model Description and Instrumentation

The inlet test program consisted of a preliminary wind tunnel test in the NASA Ames 6 × 6 ft wind tunnel, followed by a final test in the Rockwell Trisonic 7 × 7 ft blow-down facility. An intermediate test was performed at (GD/FW ETL) to refine the bleed system and test the inlet performance and distortion under static conditions. The first test conducted in the NASA Ames 6 × 6 ft wind tunnel used an 0.15 scale model consisting of a forebody, boundary-layer diverter, primary inlet, subsonic duct, compressor-face instrumentation, and remotely actuated throttle plug for the primary inlet. The compressor face instrumentation consists of 40 steady-state total pressure probes and 40 high-response probes where each pair of probes is mounted jointly in a single unit. Other total and static pressure instruments are located down the subsonic duct, along the diverter, and in the orifice plate at the rear end of the diverter bleed chamber to measure bleed flow rates. The GD/FW ETL static test used the same instrumentation as in the NASA Ames wind tunnel test.

The Rockwell Trisonic wind tunnel test was conducted in a blow-down facility with a 7 × 7 ft test section. The average run lasted between 20 and 40 s. Instrumentation was more limited in this facility and only one ring of high-response compressor-face data was taken. The ring selected for high-response data acquisition was ring 3 (which is the center ring of the five concentric ring unit), where the data were processed specifically for input into the Melick Code<sup>1</sup> for instantaneous distortion levels. A boundary-layer bleed flow plug was used to control and measure the inlet bleed flow for a portion of the test and the louvers were used for the remainder of the test. A bypass plenum and flow plug were provided to simulate the engine bypass system.

### Wind Tunnel Test Results

Figure 8 shows the major inlet performance characteristics of the F-16/79 baseline inlet (configuration 12 ramp and

Fig. 6 Mach 2.0 shock system for candidate inlet designs.

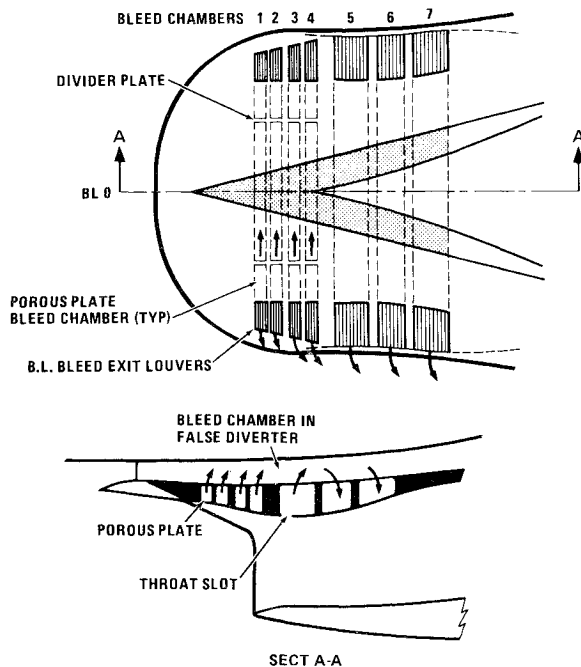
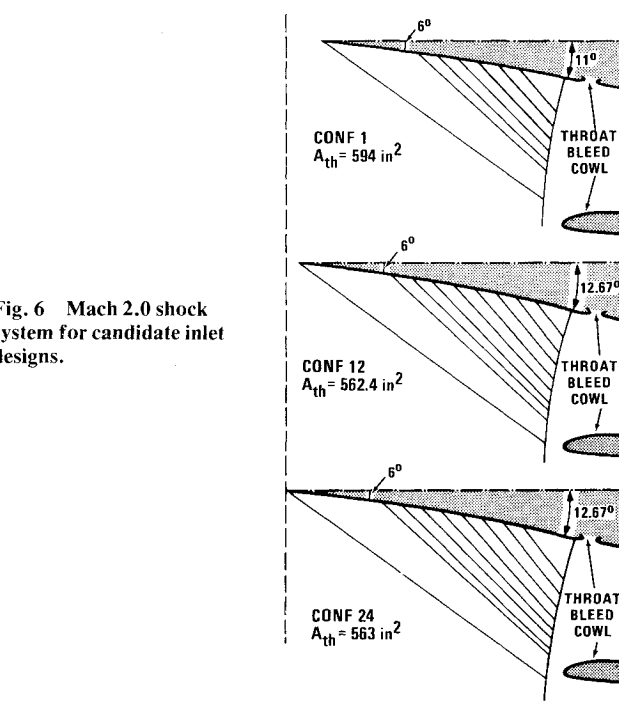


Fig. 7 Rockwell inlet model detail.

single-slot bleed through bleed chambers 5, 6, and 7) along with the corrected airflow as a function of freestream Mach number. The extended ramp and bleed system serves to increase performance levels at the higher Mach numbers when compared to the normal shock inlet of the F-16A/B. Note that the bypass valve opens up at approximately Mach 0.6 and remains open at high speeds. The pressure recovery is affected slightly at  $M=0.5-0.8$  by the opening of the bypass valve where the throat Mach number is increased with the increased bypass airflow. In addition, the throat bleed closure door starts to open at approximately the same time the bypass opens, which has some effect on recovery. Figure 8 also shows the effect of sideslip on pressure distortion to remain well below  $N_c=0.12$ , which is an upper distortion limit. This

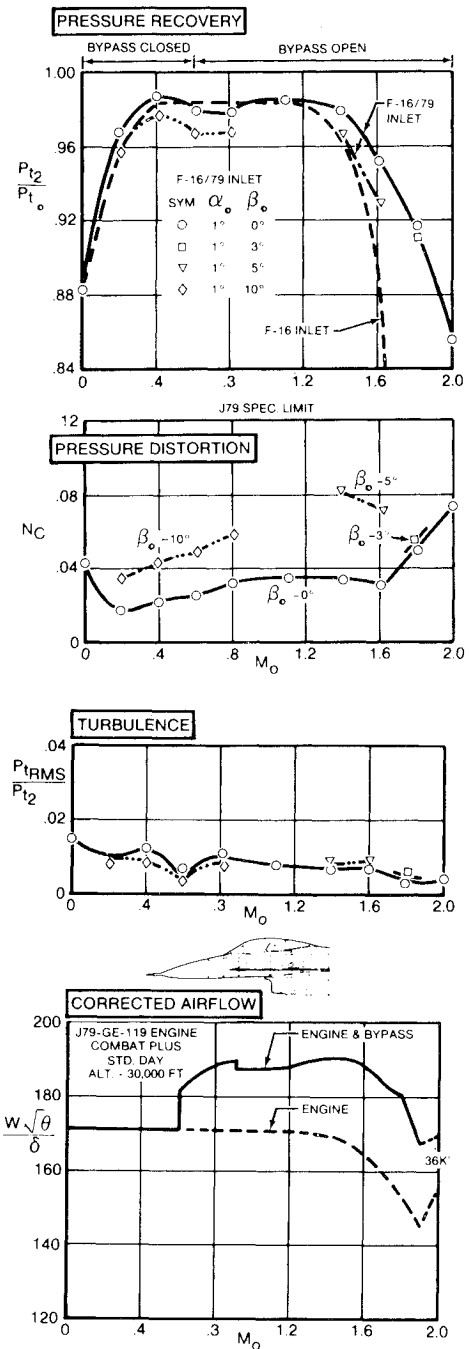


Fig. 8 F-16/79 inlet performance characteristics.

parameter is a circumferential distortion indicator, which has a limiting value of 0.12 for the J79 engine. For values of  $N_c < 0.12$  (which is a very conservative steady-state value) the distortion levels may be regarded as stall free. Flight test data indicate that the  $N_c$  limit is a very conservative number and that engine stalls are not likely to be encountered until an  $N_c$  value of at least 0.20-0.25 is encountered (see Fig. 9).

At high speeds both the NASA Ames and Rockwell test data are combined. They are shown in Fig. 10, where pressure recovery is slightly higher for the Rockwell test and the stable airflow margin is significantly increased. Two effects are responsible for this: 1) increased bleed in the Rockwell test and 2) higher Reynolds number in the Rockwell tunnel ( $1.5 \times 10^6$  vs  $9 \times 10^6$ ). The pressure recovery differentials are more substantial at higher angles of attack. Distortion is also decreased in the Rockwell test as a result of less boundary-layer interaction due to the higher Reynolds number and

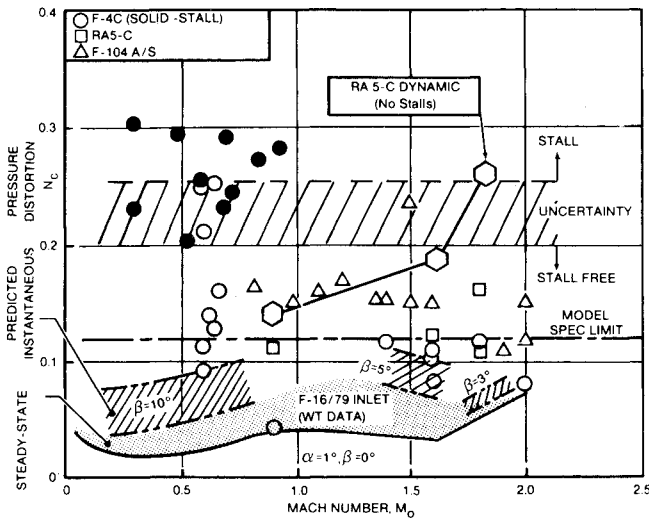
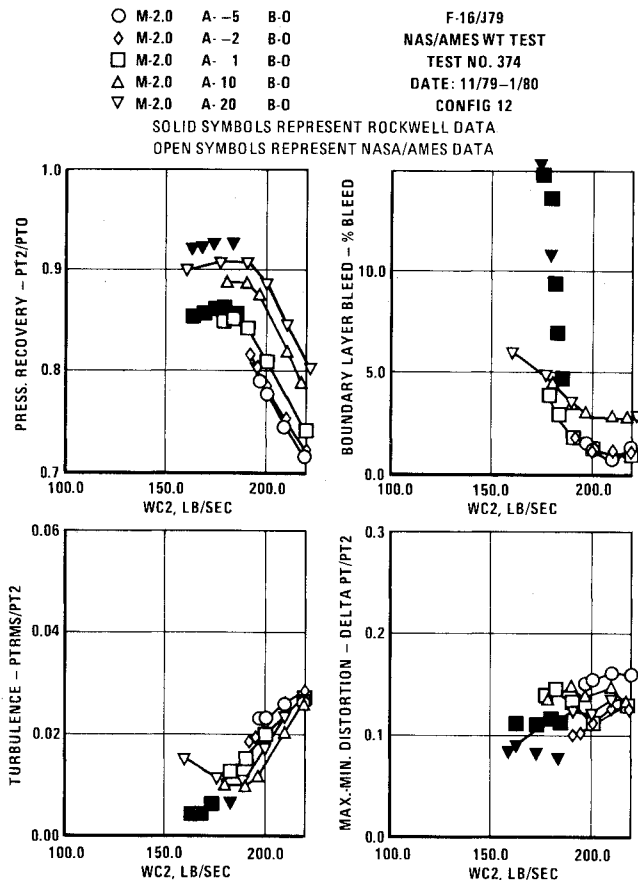


Fig. 9 Inlet pressure distortion comparison.

Fig. 10 Comparison of Rockwell and NASA Ames data at  $M_0 = 2.0$  showing the effect of angle of attack.

greater bleed. A further comparison of the variations in the bleed system is shown in Fig. 11, where performance with the porous ramp and throat slot in compared with the throat slot alone. Performance levels are not significantly changed; however, with the porous ramp the inlet is stable over a much larger airflow range, especially at Mach 1.8 and 2.0.

The subcritical stable operating range of the F-16/79 inlet at cruise flight attitude is shown in Fig. 12. At Mach 1.6 and above, the least stable operating point (indicated by the left-most value of the pressure recovery characteristic) was defined during the wind tunnel test. At duct-corrected airflows less than those indicated by this limit, the boundary

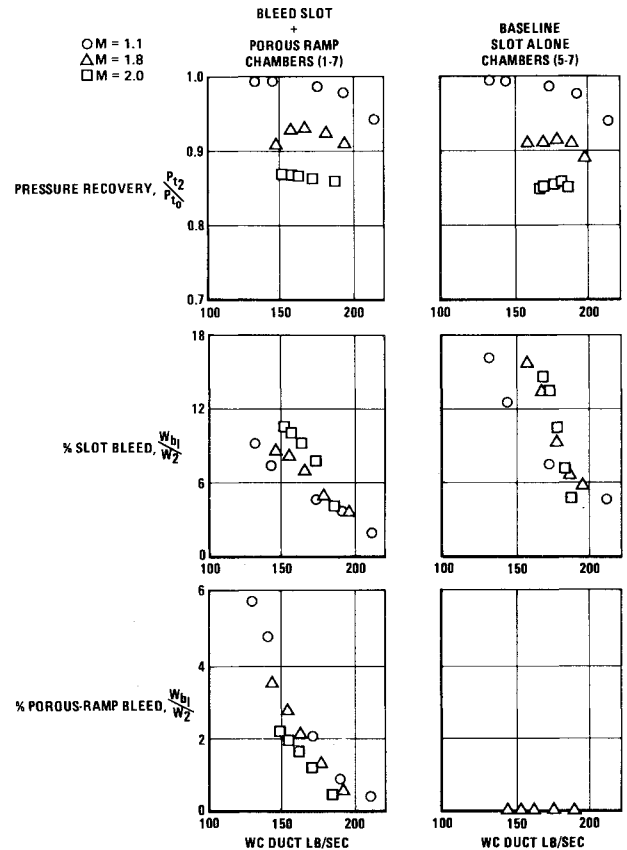


Fig. 11 Rockwell test comparing performance of different bleed arrangements.

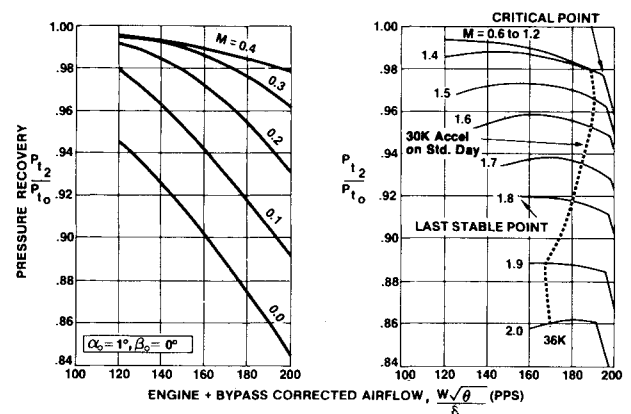


Fig. 12 Pressure recovery for F-16/79 as a function of Mach number.

layer on the compression ramp will separate, the shock system will become unstable and begin to oscillate, and the inlet will be operating in an unstable mode commonly referred to as "inlet buzz." In this mode of unstable operation, pressure recovery at the engine inlet will decrease and distortion and turbulence will increase, possibly resulting in compressor stall.

As mentioned above, the inlet operating characteristics shown in Fig. 12 apply only for cruise attitude flight. During certain aircraft maneuvers where a pushover or sidlip is imposed, the minimum stable operating airflow will be more than that shown. Limited data on the effect of maneuver were acquired during the wind tunnel tests and are shown in Fig. 13.

During low-speed flight operation, the throat static pressure is much lower than the ambient static pressure, thus

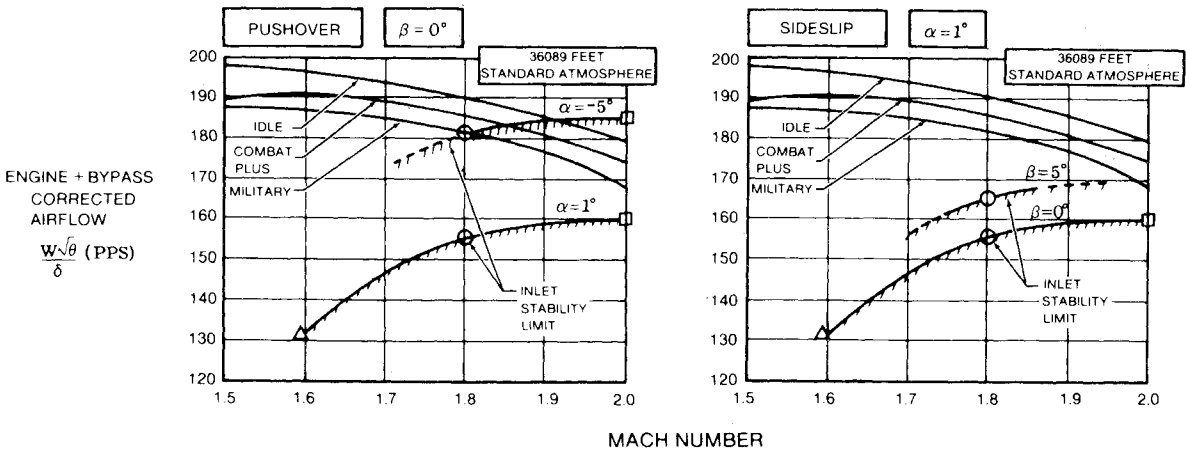
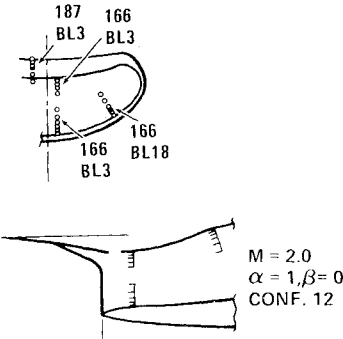
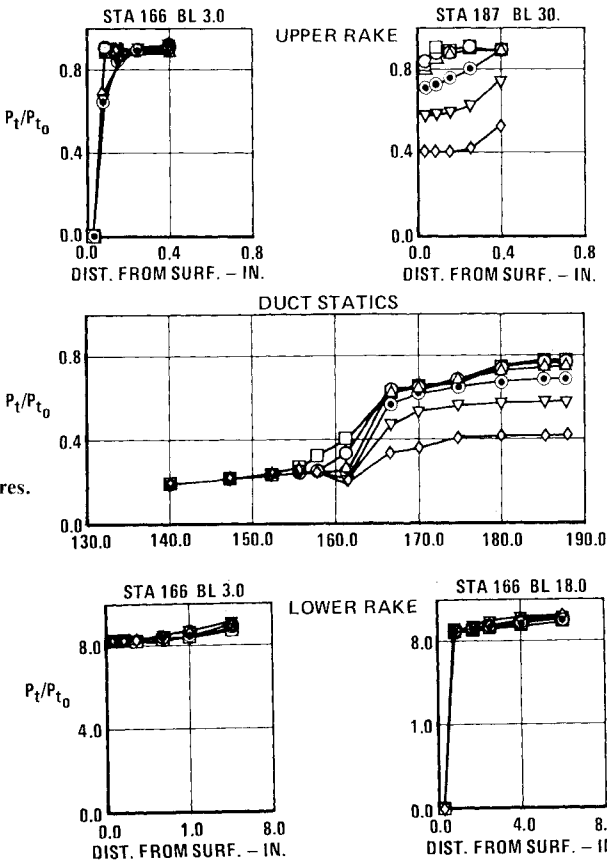
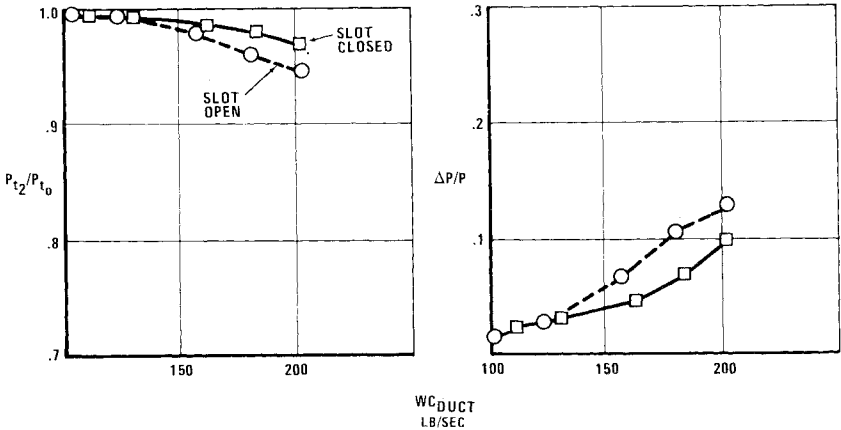


Fig. 13 Effect of aircraft maneuver on F-14/79 inlet stability limit.

Fig. 14 Effects of closed vs open throat slot at  $M=0.6$ .



RUN	WC2
□	- 218 172
○	- 218 178
△	- 218 182
●	- 218 190
▽	- 218 200
◇	- 218 219

Fig. 15 Duct static and total pressures.

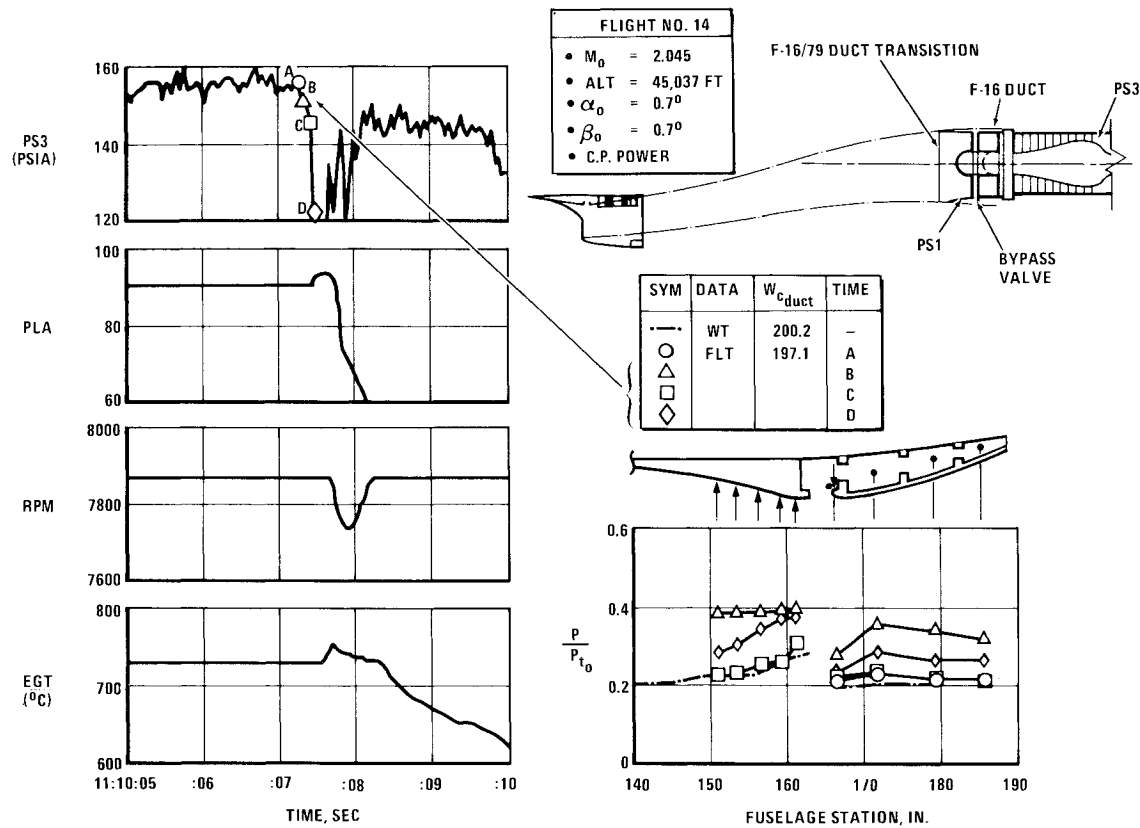


Fig. 16 Flight test data showing effect of pressure anomaly on ramp static pressure, PS3, PLA, rpm, and EGT.

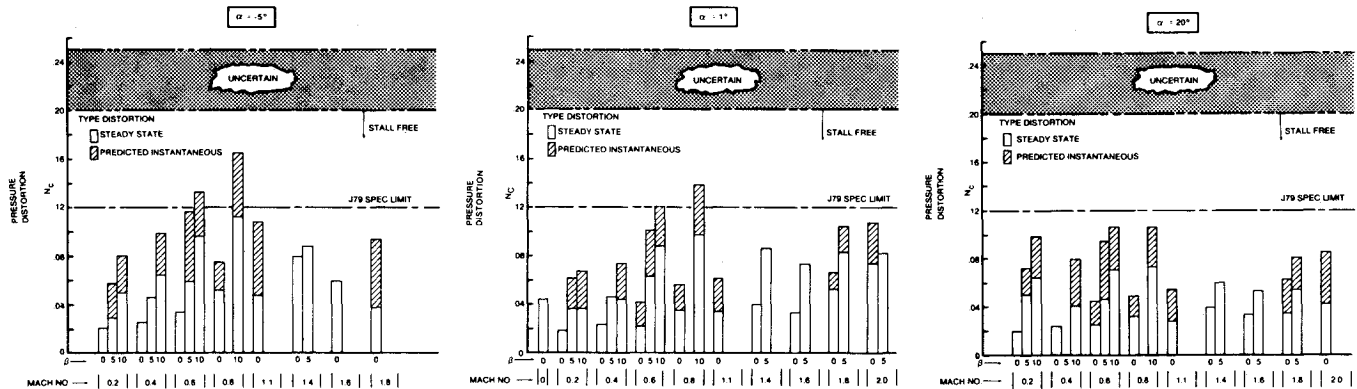


Fig. 17 Comparison of steady-state and predicted maximum instantaneous distortion at the engine inlet.

inducing a reverse flow in the BLC system. At Mach 0.6, Fig. 14 shows the effects of the reversed flow on inlet performance. Smoke tests performed at these same conditions show strong vortex flows in the corner regions of the throat slot which will degrade the performance and increase distortion. To eliminate this problem the throat slot door was added to the design.

Figure 15 shows the ramp and duct static pressures just inside the inlet at  $M=2.0$  as a function of duct airflow, where airflows greater than 190 lb/s represent supercritical flows. Also shown are the inlet throat region total pressure rake measurements. The flow is well-behaved in the inlet throat region for the subcritical flows. For the supercritical flow conditions, some separation is observed on the upper ramp surfaces, indicated by the decreased total pressure measured by the station 187 throat rake.

Flight test data at  $M=2.0$  (Fig. 16) show the inlet ramp pressure distribution along with the Rockwell wind tunnel

data. The flight test ramp data are in good agreement with the tunnel data. Using these data as a reference, time varying data were taken during a pressure anomaly (intermittent buzz condition) shown in Fig. 16). The shock movement is correlated with the PS3 compressor pressure in the engine, the power lever angle (PLA), rpm, and exhaust gas temperature (EGT) for this time sequence. The pressure in the inlet bleed cavity during this time sequence also increases as the shock moves out on the ramp, which increases the bleed through the louvers and tends to stabilize the inlet flow.

Engine Inlet Compatibility

Circumferential total pressure distortion is measured by the distortion parameter  $N_c$ . The steady-state limit value for  $N_c$  is 0.12, where Fig. 9 shows the F-16/79 distortion to be well below this limit. An historical record of the  $N_c$  pressure distortion measured in flight tests on three different aircraft

using the J79 engine is also shown in Fig. 9. Again, the F-16/79 data show a wide margin of safety.

Eight dynamic total pressure measurements were also recorded at the engine face during the wind tunnel tests. These data were used with the Melick methodology to predict maximum instantaneous total pressure distortion. This prediction is compared with steady-state results and shown across the ranges of test Mach number and maneuver attitude in Fig. 17. It is noted that the very conservative specification  $N_c$  steady-state limit value is exceeded by the instantaneous distortion only at high subsonic Mach number during severe sideslip conditions.

The results of the engine/inlet compatibility have been well demonstrated in a comprehensive flight test program during which there have been no incidents of engine stall.

### Concluding Remarks

A fixed double-ramp inlet with a throat slot bleed system has been developed for the F-16/79 derivative of the F-16A/B. Three wind tunnel tests were required to optimize the

inlet design and performance. In the subsonic and transonic Mach number range, the F-16/79 performance distortion is essentially unchanged from the F-16A/B levels. However, at Mach 2.0, performance is increased 20% and spill drag decreased 60% over the F-16A/B levels.

Various ramp/throat bleed configurations were tested where the final configuration chosen was a single transverse throat bleed slot with a bleed closure door. A bypass valve opens at approximately  $M=0.6$  and remains open at high speeds which stabilizes the inlet.

The results of the engine-inlet compatibility have been well demonstrated in a comprehensive flight test program during which there have been no incidents of engine stall.

### References

- <sup>1</sup>Ybarra, A.H. and Melick, H.C., "Computer Program Documentation, Maximum Instantaneous Distortion and Contour Map," Vought System Division, LTV Aerospace Corp., TR 2-57110/5R-SK 21, Sept. 1975.

## *From the AIAA Progress in Astronautics and Aeronautics Series...*

# **SHOCK WAVES, EXPLOSIONS, AND DETONATIONS—v. 87 FLAMES, LASERS, AND REACTIVE SYSTEMS—v. 88**

*Edited by J. R. Bowen, University of Washington,  
N. Manson, Université de Poitiers,  
A. K. Oppenheim, University of California,  
and R. I. Soloukhin, BSSR Academy of Sciences*

In recent times, many hitherto unexplored technical problems have arisen in the development of new sources of energy, in the more economical use and design of combustion energy systems, in the avoidance of hazards connected with the use of advanced fuels, in the development of more efficient modes of air transportation, in man's more extensive flights into space, and in other areas of modern life. Close examination of these problems reveals a coupled interplay between gasdynamic processes and the energetic chemical reactions that drive them. These volumes, edited by an international team of scientists working in these fields, constitute an up-to-date view of such problems and the modes of solving them, both experimental and theoretical. Especially valuable to English-speaking readers is the fact that many of the papers in these volumes emerged from the laboratories of countries around the world, from work that is seldom brought to their attention, with the result that new concepts are often found, different from the familiar mainstreams of scientific thinking in their own countries. The editors recommend these volumes to physical scientists and engineers concerned with energy systems and their applications, approached from the standpoint of gasdynamics or combustion science.

*Vol. 87—Published in 1983, 532 pp., 6×9, illus., \$30.00 Mem., \$45.00 List*  
*Vol. 88—Published in 1983, 460 pp., 6×9, illus., \$30.00 Mem., \$45.00 List*  
*Set—\$60.00 Mem., \$75.00 List*

TO ORDER WRITE: Publications Order Dept., AIAA, 1633 Broadway, New York, N.Y. 10019